Expanded View Figures

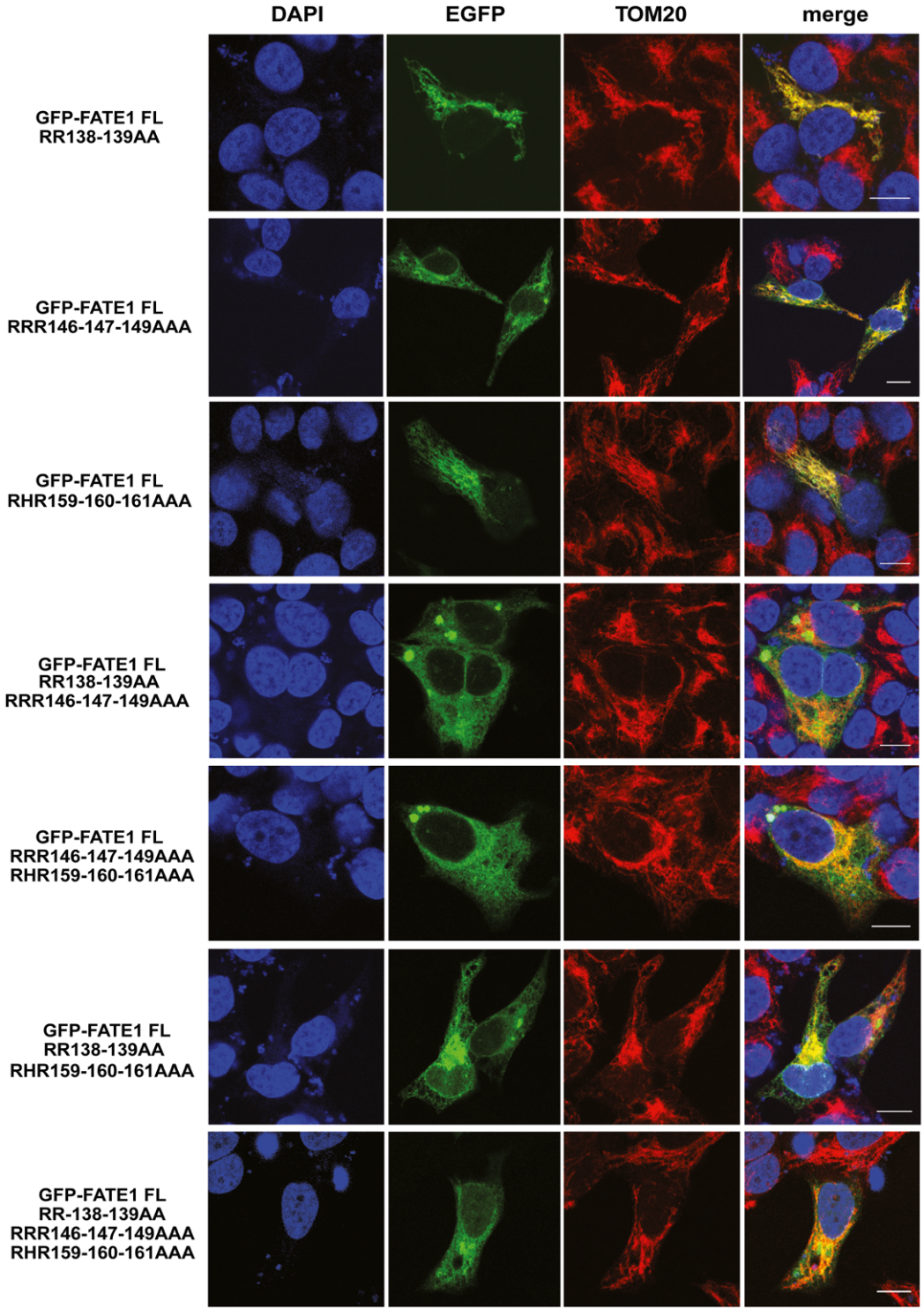

Figure EV1. Subcellular localization of EGFP-FATE1 full-length proteins bearing mutations in C-terminal domain basic residues in transfected H295R/TR SF-1 cells.
The mitochondrial marker TOM20 is stained in red and DNA in blue with DAPI. Scale bars, 10 μm.

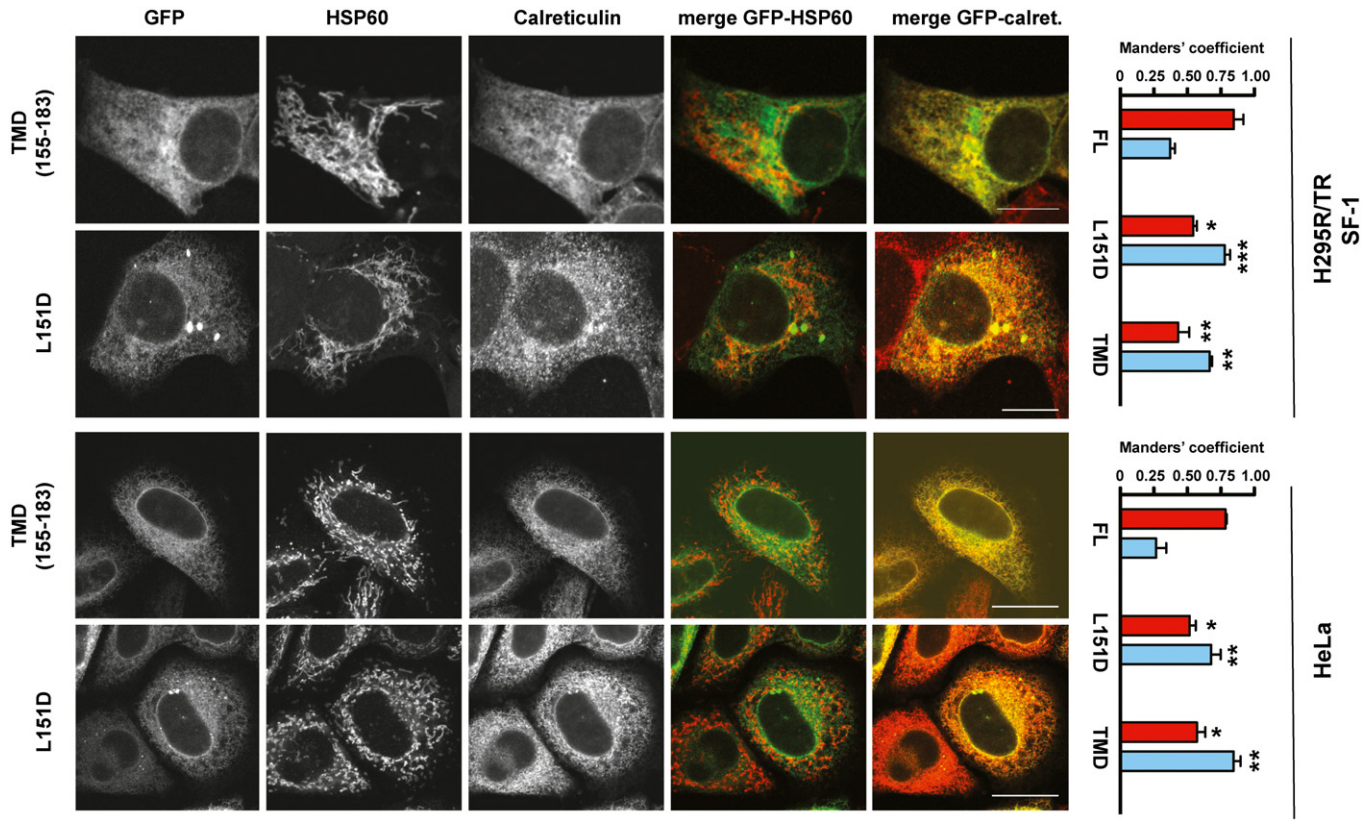

Figure EV2. Subcellular localization of EGFP-FATE1 L151D and TMD proteins in transfected H295R/TR SF-1 and HeLa cells.
HSP60 was stained as a mitochondrial marker and calreticulin as an ER marker. Manders' colocalization coefficient of both FATE1 mutants with HSP60 (red histograms) is significantly decreased compared to the full-length wild-type FATE1, while colocalization with calreticulin (pale blue histograms) is significantly increased (one-way ANOVA with Bonferroni's correction). *$P < 0.05$; **$P < 0.01$; ***$P < 0.001$. Scale bars, 10 μm.

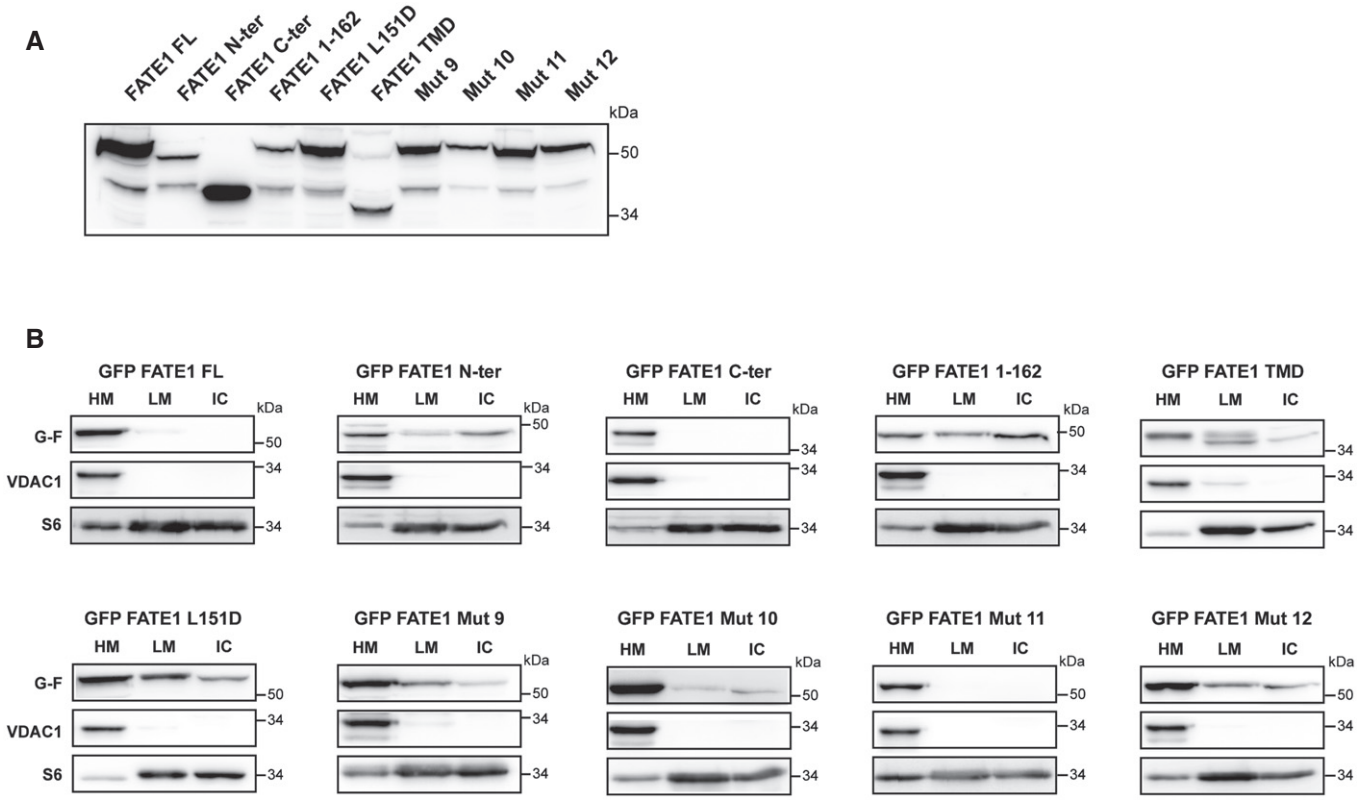

Figure EV3. Distribution of wild-type and mutant EGFP-FATE1 protein in subcellular fractions in transfected HeLa cells.

A Immunoblot showing expression of the different EGFP-FATE1 proteins in whole-cell lysates. TMD, transmembrane domain (aa 155–183). Mut 9: RR138-139AA/RRR146-147-149AAA. Mut 10: RRR146-147-149AAA/RHR159-160-161AAA. Mut 11: RR138-139AA/RHR159-160-161AAA. Mut 12: RR138-139AA/RRR146-147-149AAA/RHR159-160-161AAA.

B Immunoblot showing the distribution of transfected EGFP-FATE1 proteins (G-F) and endogenous VDAC and ribosomal protein S6 in heavy membranes (HM), light membranes (LM), and insoluble cytosolic (IC) fractions.

Source data are available online for this figure.

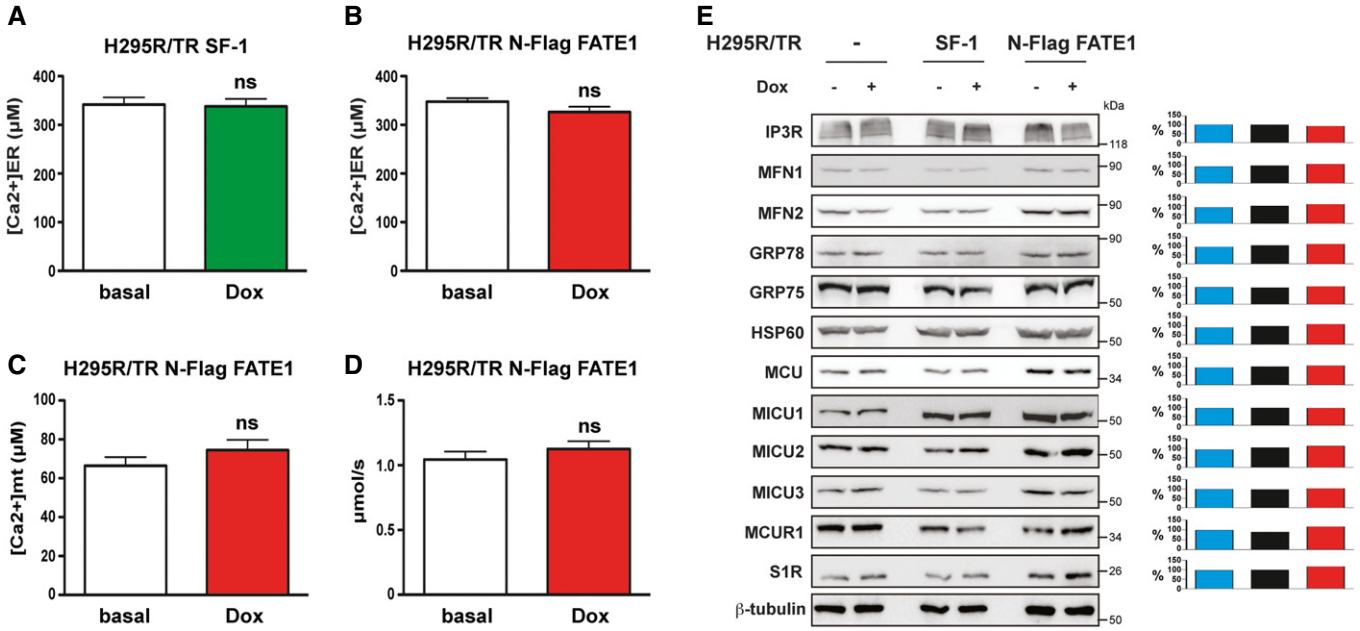

Figure EV4. Effect of FATE1 expression on Ca^{2+} concentration in ER and mitochondria after CPA treatment.

A, B H295R/TR SF-1 cells (A) and H295R/TR N-Flag FATE1 cells (B) were transduced with adenovirus for expression of ER-targeted aequorin and then treated with Dox (green or red histograms) or left untreated (white histograms) for 24 h before Ca^{2+} concentration measurement (mean ± SEM; n = 3–5 with 12 replicates/condition). ns, not significant, Mann–Whitney test.

C Mitochondrial Ca^{2+} uptake was measured after permeabilization with digitonin and CPA treatment in H295R/TR N-Flag FATE1 cells cultured in basal conditions (white histogram) or treated with Dox (red histogram) for 24 h using mitochondrial-targeted aequorin in cells perfused with 400 nM buffered Ca^{2+} (mean ± SEM; n = 3 with 12 replicates/condition). ns, not significant, Mann–Whitney test.

D Speed of mitochondrial Ca^{2+} uptake in permeabilized, CPA-treated H295R/TR N-Flag FATE1 cells (mean ± SEM; n = 3 with 12 replicates/condition). ns, not significant, Mann–Whitney test.

E Immunoblot showing protein expression in H295R/TR, H295R/TR SF-1, and H295R/TR N-Flag FATE1 cells. Cells were cultured in basal conditions or treated with Dox for 24 h. Quantification of the blot using ImageJ is shown on the right side for each protein. Blue histogram, H295R/TR cells. Black histogram, H295R/TR SF-1 cells. Red histogram, H295R/TR N-Flag FATE1 cells. Band intensity signals for the expression of each protein in Dox conditions were expressed as percentage of basal signal and normalized by the corresponding β-tubulin signal using ImageJ software.

Source data are available online for this figure.

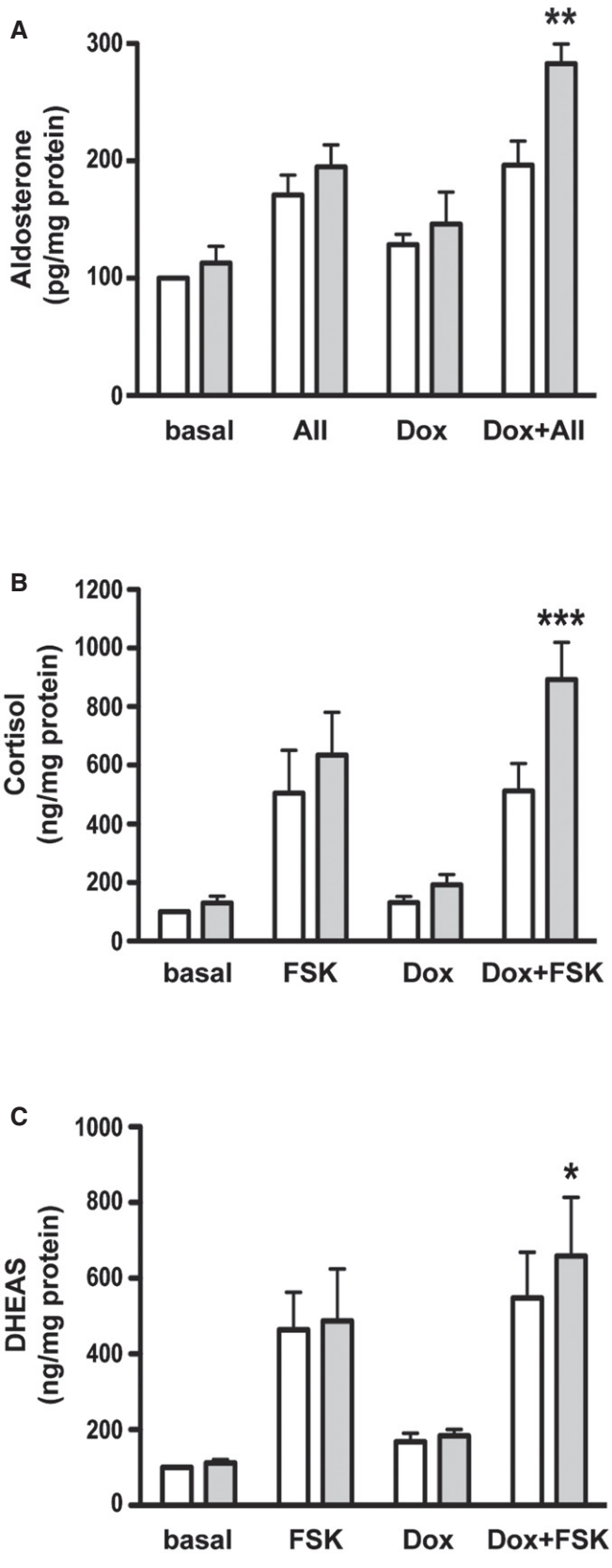

Figure EV5. Effect of FATE1 expression on steroid hormone production in H295R/TR SF-1 cells.

A–C Aldosterone (A), cortisol (B), and DHEAS (C) levels were measured in H295R/TR SF-1 cells nucleofected with control (white histograms) or FATE1-specific (gray histograms) siRNA in basal conditions or after Dox treatment. Cells were either left unstimulated (control) or stimulated with angiotensin II (AII; 10 nM) and forskolin (FSK; 10 μg/ml), respectively (mean ± SEM; n = 5 with 3 replicates/condition). ***$P < 0.001$; **$P < 0.01$; *$P < 0.05$, one-way ANOVA with Bonferroni's correction.